IJMMM International Journal of Minerals, Metallurgy and Materials 矿物冶金与材料学报（英文版）

Effect of graphene addition on the physicomechanical and tribological properties of Cu nanocomposites

Adnan I. Khdair and A. Ibrahim

Cite this article as:
Adnan I. Khdair and A. Ibrahim, Effect of graphene addition on the physicomechanical and tribological properties of Cu nanocomposites, *Int. J. Miner. Metall. Mater.*, 29(2022), No. 1, pp. 161-167. https://doi.org/10.1007/s12613-020-2183-0

View the article online at SpringerLink or IJMMM Webpage.

Articles you may be interested in

Mohammad Khosravi, Mohammad Mansouri, Ali Gholami, and Yadollah Yaghoubinezhad, Effect of graphene oxide and reduced graphene oxide nanosheets on the microstructure and mechanical properties of mild steel jointing by flux-cored arc welding, *Int. J. Miner. Metall. Mater.*, 27(2020), No. 4, pp. 505-514. https://doi.org/10.1007/s12613-020-1966-7

Tian-shun Dong, Ming Liu, Yang Feng, Guo-lu Li, and Xiao-bing Li, Microstructure and properties of a wear resistant Al–25Si–4Cu–1Mg coating prepared by supersonic plasma spraying, *Int. J. Miner. Metall. Mater.*, 27(2020), No. 9, pp. 1287-1294. https://doi.org/10.1007/s12613-019-1950-2

Zuo-li Li, Jun Zhao, Jia-lin Sun, Feng Gong, and Xiu-ying Ni, Reinforcing effect of graphene on the mechanical properties of Al_2O_3/TiC ceramics, *Int. J. Miner. Metall. Mater.*, 24(2017), No. 12, pp. 1403-1411. https://doi.org/10.1007/s12613-017-1533-z

Essam B. Moustafa and Mohammed A. Taha, Evaluation of the microstructure, thermal and mechanical properties of Cu/SiC nanocomposites fabricated by mechanical alloying, *Int. J. Miner. Metall. Mater.*, 28(2021), No. 3, pp. 475-486. https://doi.org/10.1007/s12613-020-2176-z

Mohammad Baghani, Mahmood Aliofkhazraei, and Mehdi Askari, Cu-Zn-Al_2O_3 nanocomposites:study of microstructure,corrosion,and wear properties, *Int. J. Miner. Metall. Mater.*, 24(2017), No. 4, pp. 462-472. https://doi.org/10.1007/s12613-017-1427-0

Wei Liu, You-hui Jiang, Hui Guo, Yue Zhang, Ai-min Zhao, and Yao Huang, Mechanical properties and wear resistance of ultrafine bainitic steel under low austempering temperature, *Int. J. Miner. Metall. Mater.*, 27(2020), No. 4, pp. 483-493. https://doi.org/10.1007/s12613-019-1916-4

IJMMM WeChat

QQ author group

International Journal of Minerals, Metallurgy and Materials
Volume 29, Number 1, January 2022, Page 161
https://doi.org/10.1007/s12613-020-2183-0

Effect of graphene addition on the physicomechanical and tribological properties of Cu nanocomposites

Adnan I. Khdair[1,2),✉] *and A. Ibrahim*[3)]

1) Mechanical Engineering Department, Faculty of Engineering, King Abdulaziz University, P.O. Box 80204, Jeddah, Saudi Arabia
2) Jordan University of Science and Technology, Mech. Eng. Dep., P.O. Box 3030, Irbid 2011, Jordan
3) Higher Technological Institute, Tenth of Ramadan City, Egypt
(Received: 2 June 2020; revised: 6 August 2020; accepted: 31 August 2020)

Abstract: This paper presents an experimental investigation of the mechanical and tribological properties of Cu–graphene nanosheets (GN) nanocomposites. We employed the electroless coating process to coat GNs with Ag particles to avoid its reaction with Cu and the formation of intermetallic phases. We analyzed the effect of GN content on the structural, mechanical, and tribological properties of the produced nanocomposites. Results showed that the electroless coating process is an efficient technique to avoid the reaction between Cu and C and the formation of intermetallic phases. The addition of GNs significantly improves the mechanical and tribological properties of Cu nanocomposites. However, the addition of GNs needs to be done carefully because, after a certain threshold value, the mechanical and tribological properties are negatively affected. The optimum GN content is determined to be 0.5vol%, at which hardness, wear rate, and coefficient of friction are improved by 13%, 81.9%, and 49.8%, respectively, compared with Cu nanocomposites. These improved properties are due to the reduced crystallite size, presence of GNs, and homogenous distribution of the composite constituents.

Keywords: copper; graphene nanosheets; coating; mechanical properties; wear

1. Introduction

The applications of nanocomposite materials significantly increased in the past two decades because of the improvement of their properties [1–4]. For example, we achieved nanocomposite materials with excellent mechanical properties and good electrical and thermal properties, which make them a good choice for electrodes working at elevated temperatures [3]. Another important advantage is that the combination of these properties can be tailored by adjusting the manufacturing parameters, such as reinforcement weight fraction [5], and the properties of the constituents [6–7]. Despite the progress achieved in the field of metal matrix nanocomposites, knowledge of the optimized weight fraction of the reinforcement phases that achieve a combination of good mechanical and tribological properties is still lacking.

One of the most interesting natural metals is copper (Cu) because of its excellent electrical and thermal properties combined with good mechanical properties [8–10], which make it and its alloys excellent candidates for many structural applications. Several manufacturing processes to produce Cu-based nanocomposites have been presented in the literature. Among these techniques, mechanical alloying is the most efficient technique that achieves the homogenous distribution of the reinforcement particles in the Cu matrix [11–13]. During this process, the repeated fracture and welding actions during milling initiate the formation of a metastable phase, which is beneficial to the alloying process [13]. The alloying of Cu, which has a body centered cubic (bcc) crystal structure, with metals that have a face centered cubic (fcc) crystal structure has been presented in the literature for many years because of the difficulties encountered in dissolving these metals, resulting in an alloy with improved properties [14]. The alloying of Cu with different metals, including Nb, Ag, Ta, Cr, and Fe, which results in better mechanical properties of the produced composite, has been presented in the literature [15]. Cu–Fe has superior mechanical and magnetic properties with relatively low cost compared with other alloying elements [16–17]. Wu *et al.* [18] and Qu *et al.* [19] manufactured Cu–Fe alloy using the vacuum induction melting process at different processing temperatures. They concluded that the strength of the alloy is higher than that of the plain Cu metal and dependent on the processing temperature. The high-pressure torsion process was applied to produce Cu–Fe alloy with a fiber-like shape [20]. The mechanical alloying process was also applied to produce Cu–20wt%Fe alloy with improved strength [21].

To further improve the mechanical and wear properties of Cu-based matrix composites, reinforcements have been added to manufacture Cu-based nanocomposites. Among sev-

✉ Corresponding author: Adnan I. Khdair E-mail: akhdair@kau.edu.sa, akhdair@just.edu.jo
© University of Science and Technology Beijing 2022

eral available reinforcements, graphene nanosheets (GNs) have superior mechanical and electrical properties [22–24]. Several studies reported the production of several nanocomposites reinforced with GNs with improved mechanical and wear properties [25–28].

The objective of this study is to manufacture Cu–GN nanocomposites using the mechanical alloying technique and characterize their mechanical and tribological properties. We coated GNs with Ag particles using the electroless coating process to avoid the reaction between GNs and Cu. We analyzed the effect of GN content on the structural, mechanical, and wear properties of Cu–GN nanocomposites. We investigated the different strengthening mechanisms of this nanocomposite and highlighted the optimum GN content to achieve improved mechanical and tribological properties.

2. Experimental

We employed several kinds of chemicals to *in situ* manufacture Cu particles, including silver nitrate ($AgNO_3$), copper sulfate ($CuSO_4$), potassium sodium tartrate ($KNaC_4H_4O_6\cdot 4H_2O$), formaldehyde (CH_2O), sodium hydroxide (NaOH), and ammonia (NH_3). Some of these chemicals were also used for coating purposes. With the aid of the electroless deposition process, we produced Cu powders with 99.9% purity and 90 nm average size as the main matrix. We used iron powder with 99.9% purity and 15 μm average size as the second matrix to prepare the Cu matrix with a weight concentration of 90:10. We used GNs with 99.99% purity and 90 nm average size as the reinforcement.

We employed four steps to manufacture Cu nanocomposite reinforced with GNs. First, we *in situ* manufactured nanosized Cu powder using the electroless plating process. A bath of 170 g/L $KNaC_4H_4O_6\cdot 4H_2O$, 35 g/L $CuSO_4$, 50 g/L NaOH, and 140 mL/L CH_2O was used to precipitate Cu nanoparticles. After the reaction was completed, we washed the precipitated Cu nanoparticles using distilled water and dried them at 110°C for 1 h. Second, we applied the electroless plating process again to coat GNs with Ag particles (approximately 5 nm thickness) to avoid its reaction with Cu. We used Ag particles to coat GNs because it adheres to GNs better than other particles, as reported in our previous study and others in the literature [15,23–24]. To do so, we prepared a solution of 10vol% NaOH, mixed it with GNs, and stirred it for 1 h. Then, we removed the GNs from the bath and immersed it in acetone to eliminate contaminants on the surface of GNs that might hinder the precipitation of Ag. We dried GNs at 110°C for 1 h. Afterward, we submerged GNs in a new bath of 3 g/L $AgNO_3$ and 300 mL/L CH_2O and adjusted the pH value to 12 using ammonia. Once CH_2O was added to the chemical bath, the reaction was initiated and the Ag nanoparticles were precipitated over GNs. The GNs were immersed in the bath for 10 min, and a magnetic stirrer was used to keep the GNs moving in the bath at room temperature. The GNs were again filtrated, washed using acetone, and dried at 110°C for 1 h. Third, we employed the high-energy ball milling process to mix Cu and GNs after coating to prepare the nanocomposite with the predefined weight percent. Stainless steel vial and balls with a diameter of 10 mm were used to mix the materials with a fixed ball-to-powder volume ratio of 15:1 and milling speed of 200 r/min. The mixture was milled for 20 h under the same condition with 10 min stop intervals every 5 h to avoid heat generation during milling, as proposed by Wagih *et al.* [29]. Finally, we compacted the mixed powders in a die preheated up to 850°C under an argon atmosphere at 700 MPa. We maintained the heat of the die during the compacting process and after compaction for 20 min. Then, the die was cooled down in an open atmosphere.

We employed the X-ray diffraction (XRD) technique to evaluate the structural changes in the prepared powder using the Bruker advanced X-ray diffractometer within the scanning range of 10° to 80°. We employed the William–Hall equation [30] to calculate the crystallite size and the equation proposed by Danilchenko *et al.* [31] to calculate the lattice strain from the recorded XRD data. We used a scanning electron microscope equipped with energy-dispersive X-ray spectrometers to evaluate the morphological changes of the prepared powders and the compacted samples.

We used Archimedes' immersion principle to evaluate the densification process of the produced nanocomposites. We used the rule of mixtures to calculate the theoretical density that was used to compute the relative density of the produced samples. We used the Vickers microhardness test to evaluate the mechanical properties of the produced samples following the ASTM E92 standard. Before the hardness test, the samples were polished using sandpapers with different grit sizes, followed by cloth and diamond paste polishing. The indentation load of 50 N was applied to the surface of the samples with 15 s dual time. At least seven indentations were performed for each sample, and the average value was determined.

We applied the sliding wear and pin-on-disk tests following the ASTM G77–98 standard to evaluate the wear resistance of the prepared samples. A steel disk with a diameter of 73 mm and surface roughness of 60 μm was used to wear the pins prepared from the manufactured materials with a diameter of 12 mm. We applied four different loads, i.e., 5, 10, 15, and 20 N, at a constant sliding distance of 200 m and constant speed of 1 m/s. The wear rates were calculated by weighting the resulting debris after sliding for 200 m. The coefficient of friction was evaluated using the measured friction torque during sliding.

3. Results and discussion

The XRD patterns of the Cu matrix reinforced with different GN contents are shown in Fig. 1. The Bragg peaks of Cu, Ag, and C appear clearly for all of the samples without any other peak. Typically, milling of Cu and GNs without coating results in the formation of intermetallic phases because of the reaction between Cu and C [32]. In this study, using the electroless coating process, we demonstrated that no intermetallic phases are formed during the milling process.

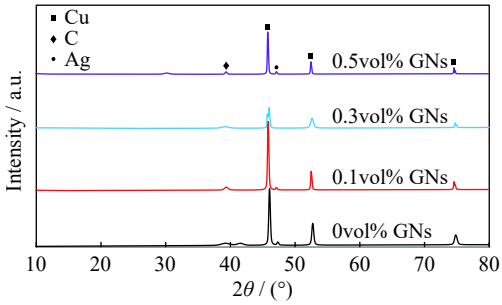

Fig. 1. XRD patterns of the composite powder reinforced with different GN contents.

Table 1 shows the evolution of the crystallite size of Cu–GN nanocomposites with different GN contents. The crystallite size decreases with the increase in GN content by up to 0.5vol%, reaching 625.69 nm compared with 771.58 nm for the Cu matrix, i.e., a decrease of 19%. Crystallite size reduction is due to the presence of GNs in the microstructure, which creates crystal defects and dislocations [33–35]. Crystallite size reduction indicates that grain refinement occurred in the samples [35]. Crystallite size reduction leads to a decrease in particle size, as shown in Fig. 2. The average particle size of the samples containing 0.3vol% and 0.5vol% GNs is 2.32 and 0.915 μm, respectively. The lattice strain increases with the increase in GN content because of the high stored internal strain in Cu particles activated by the penetration of GNs into the lattice structure of Cu, resulting in the formation of distortions.

Table 1. Crystallite size and lattice strain of the nanocomposite powder

GN content / vol%	Crystallite size / nm	Lattice strain / %
0	771.58	0.3648
0.1	707.49	0.3242
0.3	667.64	0.3055
0.5	625.69	0.2841

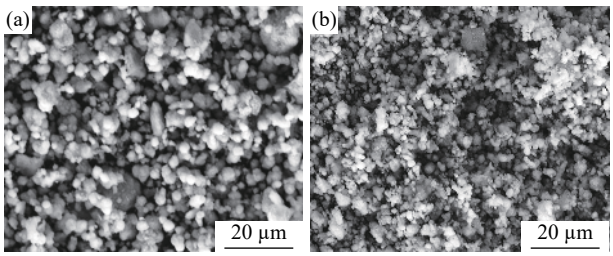

Fig. 2. Scanning electron microscopy (SEM) micrographs of the nanocomposite powder: (a) 0.3vol% GNs and (b) 0.5vol% GNs.

Fig. 3 shows the microstructure of the samples containing 0.1vol%, 0.3vol%, and 0.5vol% GNs, highlighting the presence of micropores and the distribution of GNs. Fig. 3(a) and (b) show the good distribution of GNs in the samples without any agglomeration. However, in the sample with 0.5vol% GNs, agglomeration of GNs is observed in several regions of the sample. Micropores are observed in all of the samples. The presence of micropores is due to the entrapment of air between particles during consolidation, which is observed in nearly all metal matrix nanocomposites [36–38]. Moreover, the irregular shape of GNs (i.e., plate shape) increases the tendency to entrap air during consolidation. Furthermore, the large difference between surface energies of GNs and Cu contributes to the formation of voids. Notably, the amount of voids in the sample increases with the increase in GN content. The increase in the amount of voids with the increase in GN content is attributed to the agglomeration of GNs with irregular shapes that induce the entrapment of air bubbles, as shown in Fig. 3(c).

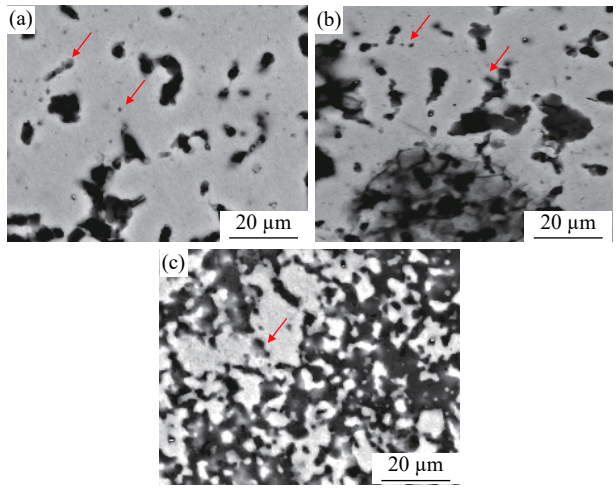

Fig. 3. SEM micrographs of the nanocomposite after consolidation: (a) 0.1vol% GNs, (b) 0.3vol% GNs, and (c) 0.5vol% GNs.

Fig. 4 shows the energy-dispersive X-ray spectroscopy and mapping analysis of the Cu–0.5vol%GN nanocomposite after consolidation to examine the composition of the sample and the elemental distribution of the contents. The figure shows that the sample contains only Cu, Ag, and C without any contaminant, which proves the validity of the manufacturing method. Moreover, the figure shows the excellent distribution of the constituent elements in the sample without any agglomeration.

Fig. 5 summarizes the relative density of the Cu–GN nanocomposites with different GN contents. The relative density is less than 100% for all of the considered samples, even for the Cu matrix, because of the formation of voids during the consolidation of Cu powders with different sizes. The relative density decreases with the increase in GN content for all of the considered samples. However, the decrease rate at low GN content (i.e., less than 0.5vol%) is smaller than the decrease rate at high GN content. For example, the relative density decreases from 98.3% for the Cu matrix to 98% for the Cu–0.1vol%GN nanocomposite. However, the density decreases to 97.3% for the Cu–0.5vol%GN nanocomposite, i.e., a decrease rate of 1.017%. These results are consistent with the microstructural observations (Fig. 3). The increased agglomeration size of GNs in samples with 0.5vol% GN content is the main reason for the decrease in relative density because of the entrapment of a large amount of air between GN flakes during consolidation and the diffi-

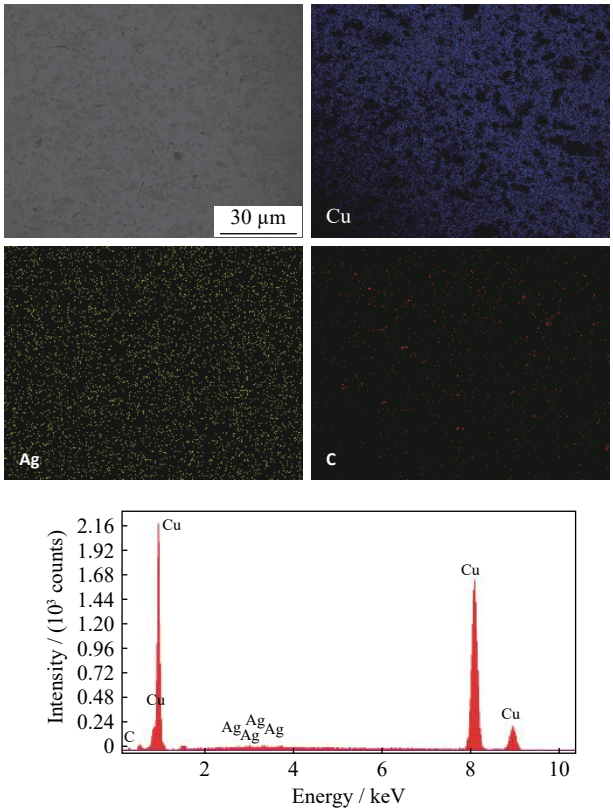

Fig. 4. Energy-dispersive X-ray spectroscopy and mapping analysis of the Cu–0.5vol%GN nanocomposite.

culties encountered during compression of GN flakes, which have high mechanical properties [39–41]. However, for samples with low GN content, the excellent dispersion of GNs helps fill the voids between Cu grains, resulting in improved relative density.

Fig. 6 presents the average value of the microhardness of Cu–GN nanocomposites with different GN contents. The

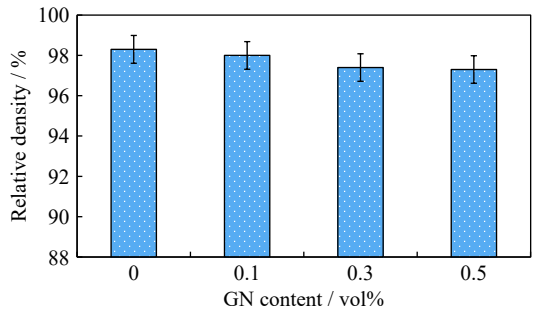

Fig. 5. Relative density of the Cu–GN nanocompositeswith different GN contents.

hardness increases even with the addition of a small amount of GNs. This improvement is due to the crystallite size reduction (see Fig. 3) and the superior mechanical properties of GNs. Increasing the GN content further improves the hardness, reaching HV 516.5 for the sample with 0.5vol% GNs. The homogeneous distribution of GNs (see Fig. 6) also helps improve the hardness [42–43]. This finding indicates the dependence of hardness on the distribution of GNs and the crystallite size of the matrix. Table 2 shows the variation of the hardness of Cu–GN composites coated with Ag in this

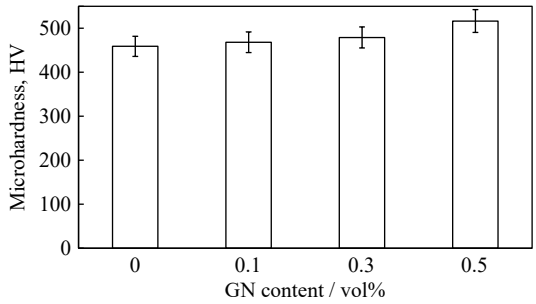

Fig. 6. Microhardness of the Cu–GN nanocomposites with different GN contents.

Table 2. Variation of the microhardness of the samples used in this study and those reported in the literature

Ref.	Material	Process	Hardness
This study	Cu	Coating with Ag + milling + compaction	HV 459.0
	Cu–0.1vol%GNs		HV 468.1
	Cu–0.3vol%GNs		HV 479.1
	Cu–0.5vol%GNs		HV 516.5
[44]	Cu	Milling + hot pressing	HV 76
	Cu–3wt%GNs		HV 84
	Cu–5wt%GNs		HV 92
	Cu–8wt%GNs		HV 104
	Cu–12wt%GNs		HV 94
[45]	Cu	Molecular-level mixing + spark plasma sintering	1.0 GPa
	Cu–0.2wt%GNs		1.50 GPa
	Cu–0.4wt%GNs		1.70 GPa
	Cu–0.6wt%GNs		1.75 GPa
	Cu–0.8wt%GNs		1.70 GPa
	Cu–2wt%GNs		1.50 GPa
	Cu–4wt%GNs		1.25 GPa
[46]	Cu	Direct current electrodeposition	1.55 GPa
	Cu–GNs		2.30 GPa

study and Cu–GN composites without coating in previous studies. The table shows that the improvement rate of the results obtained in this study is higher than those reported in the literature.

Fig. 7 shows the variation of the wear rates of Cu–GN nanocomposites with different applied loads. With the increase in the applied load, the material removal rate increases because of the higher penetration of the indenter into the sample during sliding [47]. The significance of the load is reduced by the addition of GNs because of the decreased plasticity of the material. The wear test is analogous to the indentation test. Therefore, increasing the load increases the material deformation under the indenter up to the plastic deformation limit at which more material is removed; hence, the wear rate is increased. This phenomenon was previously reported for different materials [48].

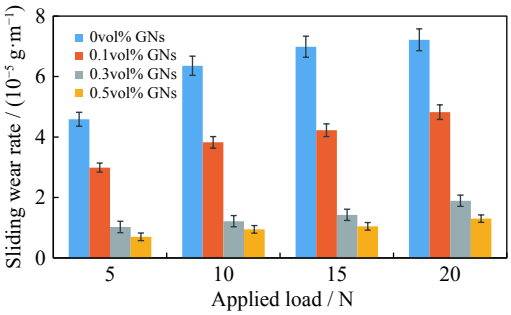

Fig. 7. Wear rate of the Cu–GN nanocomposites with different applied loads.

The addition of a small amount of GNs (i.e., 0.1vol%) to the Cu matrix reduces the wear rate at 20 N from 7.215×10^{-5} to 4.821×10^{-5} g/m, i.e., a reduction in the wear rate by 33.2%. Because of the nature of the wear test that requires the penetration of the indenter into the material surface, the hardness of the material plays a critical role. Increasing the hardness increases the resistance of the material to penetration, which improves the wear rate. Moreover, the presence of GNs under the indenter impedes the removal of more material because of its excellent mechanical properties. Furthermore, the homogenous distribution of GNs inside the matrix enables the uniform removal of the material without any possibility of excess removal in some regions [48–50]. Increasing the GN content reduces the wear rate at 0.5vol% to 1.301×10^{-5} g/m, i.e., a reduction in the wear rate by 81.9%. This significant improvement is due to the increased GN content, reduced crystallite size, and homogenous distribution of GNs in the matrix.

Fig. 8 shows the variation of the coefficient of friction of the Cu–GN nanocomposites with different applied loads. The coefficient of friction increases with the increase in applied load, i.e., for Cu matrix, the coefficient of friction increases from 0.428 at 5 N to 0.615 at 20 N. This increase is due to the increased plastic deformation because of the higher penetration of the indenter, which increases the contact area during sliding, therefore increasing the coefficient of friction. The same trend is observed for all of the tested samples with less significance when the GN content increases. The coefficient of friction is highly influenced by the addition of GNs. It decreases from 0.615 for the Cu matrix to 0.482 for the Cu–0.1vol%GN nanocomposite at 20 N, i.e., a decrease of 21.9%. This trend is consistent with the wear rate curves (see Fig. 8). The minimum coefficient of friction is achieved for the sample with 0.5vol% GNs at all of the considered loads, which make it the optimum nanocomposite. The coefficient of friction is reduced to 0.309, i.e., a decrease of 49.8%.

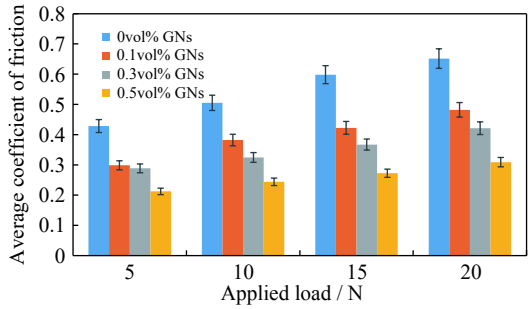

Fig. 8. Coefficient of friction of the Cu–GN nanocomposites with different applied loads.

4. Conclusions

We successfully employed electroless coating and powder metallurgy to manufacture Cu–GN nanocomposites with improved mechanical and tribological properties. We coated GNs with Ag particles to avoid its reaction with Cu and the formation of intermetallic phases. We analyzed the effect of GN content on the microstructural, mechanical, and tribological properties of Cu–GN nanocomposites. On the basis of the results, we can conclude that.

(1) The addition of GNs significantly improves the mechanical and tribological properties of Cu nanocomposites. However, the addition of GNs needs to be done carefully because, after a certain threshold value (i.e., in this study, the threshold value is 0.5vol% GNs), the mechanical and tribological properties are negatively affected.

(2) We achieved a material with good density at 0.5vol% GNs with reduced micropores. Because the GNs are coated with Ag, which improves the morphology and wettability of metals, the possibility of the formation of voids during consolidation is reduced.

(3) We achieved improved mechanical properties, with the maximum hardness of HV 516.5 for the sample containing 0.5vol% GNs compared with HV 459 for the Cu sample without GNs. This improvement is due to the reduced crystallite size, presence of GNs, and homogeneous distribution of the composite constituents.

(4) The wear rate is reduced by 81.9% and the coefficient of friction is reduced by 49.8% for the sample with 0.5vol% GN content compared with the Cu sample without GNs. However, when the GN content exceeds this threshold value, the tribological properties decrease. Finally, for the material system considered in this study, we conclude that Cu–0.5%GNs has the best mechanical and tribological properties.

Acknowledgements

This project was funded by the Deanship of Scientific Research (DSR) at King Abdulaziz University, Jeddah, under grant No. G: 455-135-1440. The authors, therefore, acknowledge with thanks DSR for technical and financial support.

Conflict of Interest

The authors declare no conflict of interest.

References

[1] A. Wagih and A. Fathy, Experimental investigation and FE simulation of nano-indentation on Al–Al_2O_3 nanocomposites, *Adv. Powder Technol.*, 27(2016), No. 2, p. 403.

[2] A. Fathy, O. El-Kady, and M.M.M. Mohammed, Effect of iron addition on microstructure, mechanical and magnetic properties of Al-matrix composite produced by powder metallurgy route, *Trans. Nonferrous Met. Soc. China*, 25(2015), No. 1, p. 46.

[3] A. Wagih, A. Fathy, and T.A. Sebaey, Experimental investigation on the compressibility of Al/Al_2O_3 nanocomposites, *Int. J. Mater. Prod. Technol.*, 52(2016), No. 3/4, art. No. 312.

[4] H.P. Tsui, J.C. Hung, K.L. Wu, J.C. You, and B.H. Yan, Fabrication of a microtool in electrophoretic deposition for electrochemical microdrilling and *in situ* micropolishing, *Mater. Manuf. Process.*, 26(2011), No. 5, p. 740.

[5] A. Fathy, A. Wagih, M.A. El-Hamid, A. Hassan, Effect of mechanical milling on the morphologyand structural evaluation of Al–Al_2O_3 nanocomposite powders, *Int. J. Eng.*, 27(2014), No. 4, p. 625.

[6] A. Wagih, A. Fathy, D. Ibrahim, O. Elkady, and M. Hassan, Experimental investigation on strengthening mechanisms in Al–SiC nanocomposites and 3D FE simulation of Vickers indentation, *J. Alloys Compd.*, 752(2018), p. 137.

[7] A.M. Sadoun and A. Fathy, Experimental study on tribological properties of Cu–Al_2O_3 nanocomposite hybridized by graphene nanoplatelets, *Ceram. Int.*, 45(2019), No. 18, p. 24784.

[8] A. Wagih and A. Fathy, Experimental investigation and FE simulation of spherical indentation on nano-alumina reinforced copper-matrix composite produced by three different techniques, *Adv. Powder Technol.*, 28(2017), No. 8, p. 1954.

[9] Y.X. Tang, X.M. Yang, R.R. Wang, and M.X. Li, Enhancement of the mechanical properties of graphene–copper composites with graphene-nickel hybrids, *Mater. Sci. Eng. A*, 599(2014), p. 247.

[10] M.S. Abd-Elwahed and A.F. Meselhy, Experimental investigation on the mechanical, structural and thermal properties of Cu–ZrO_2 nanocomposites hybridized by graphene nanoplatelets, *Ceram. Int.*, 46(2020), No. 7, p. 9198.

[11] A. Wagih, Mechanical properties of Al–Mg/Al_2O_3 nanocomposite powder produced by mechanical alloying, *Adv. Powder Technol.*, 26(2015), No. 1, p. 253.

[12] M.A. Eltaher, A Wagih, A. Melaibari, A. Fathy, and G. Lubineau, Effect of Al_2O_3 particles on mechanical and tribological properties of Al–Mg dual-matrix nanocomposites, *Ceram. Int.*, 46(2020), No. 5, p. 5779.

[13] A. Fathy, A. Wagih, and A. Abu-Oqail, Effect of ZrO_2 content on properties of Cu–ZrO_2 nanocomposites synthesized by optimized high energy ball milling, *Ceram. Int.*, 45(2019), No. 2, p. 2319.

[14] D.G. Kim, G.S. Kim, S.T. Oh, and Y.D. Kim, The initial stage of sintering for the W–Cu nanocomposite powder prepared from W–CuO mixture, *Mater. Lett.*, 58(2004), No. 5, p. 578.

[15] P.P. Macrí, S. Enzo, N. Cowlam, R. Frattini, G. Principi, and W.X. Hu, Mechanical alloying of immiscible Cu70TM30 alloys (TM = Fe, Co), *Philos. Mag. B*, 71(1995), No. 2, p. 249.

[16] A. Fathy, Investigation on microstructure and properties of Cu–ZrO_2 nanocomposites synthesized by *in situ* processing, *Mater. Lett.*, 213(2018), p. 95.

[17] L.T. Kong and B.X. Liu, Distinct magnetic states of metastable fcc structured Fe and Fe–Cu alloys studied by *ab initio* calculations, *J. Alloys Compd.*, 414(2006), No. 1-2, p. 36.

[18] Z.W. Wu, J.J. Liu, Y. Chen, and L. Meng, Microstructure, mechanical properties and electrical conductivity of Cu–12wt%Fe microcomposite annealed at different temperatures, *J. Alloys Compd.*, 467(2009), No. 1-2, p. 213.

[19] L. Qu, E.G. Wang, X.W. Zuo, L. Zhang, and J.C. He, Experiment and simulation on the thermal instability of a heavily deformed Cu–Fe composite, *Mater. Sci. Eng. A*, 528(2011), No. 6, p. 2532.

[20] M. Shaat, A. Fathy, and A. Wagih, Correlation between grain boundary evolution and mechanical properties of ultrafine-grained metals, *Mech. Mater.*, 143(2020), art. No. 103321.

[21] A.I. Khdair and A. Fathy, Enhanced strength and ductility of Al–SiC nanocomposites synthesized by accumulative roll bonding, *J. Mater. Res. Technol.*, 9(2020), No. 1, p. 478.

[22] A.K. Geim and K.S. Novoselov, The rise of graphene, *Nat. Mater.*, 6(2007), No. 3, p. 183.

[23] S.C. Tjong, Recent progress in the development and properties of novel metal matrix nanocomposites reinforced with carbon nanotubes and graphene nanosheets, *Mater. Sci. Eng. R: Rep.*, 74(2013), No. 10, p. 281.

[24] A. Nieto, A. Bisht, D. Lahiri, C. Zhang, and A. Agarwal, Graphene reinforced metal and ceramic matrix composites: A review, *Int. Mater. Rev.*, 62(2017), No. 5, p. 241.

[25] K. Chu, X.H. Wang, Y.B. Li, D.J. Huang, Z.R. Geng, X.L. Zhao, H. Liu, and H. Zhang, Thermal properties of graphene/metal composites with aligned graphene, *Mater. Des.*, 140(2018), p. 85.

[26] K. Chu, F. Wang, X.H. Wang, and D.J. Huang, Anisotropic mechanical properties of graphene/copper composites with aligned graphene, *Mater. Sci. Eng. A*, 713(2018), p. 269.

[27] K. Chu, F. Wang, Y.B. Li, X.H. Wang, D.J. Huang, and Z.R. Geng, Interface and mechanical/thermal properties of graphene/copper composite with Mo_2C nanoparticles grown on graphene, *Composites A: Appl. Sci. Manuf.*, 109(2018), p. 267.

[28] K. Chu, F. Wang, X.H. Wang, Y.B. Li, Z.R. Geng, D.J. Huang, and H. Zhang, Interface design of graphene/copper composites by matrix alloying with titanium, *Mater. Des.*, 144(2018), p. 290.

[29] A. Wagih, A. Fathy, and A.M. Kabeel, Optimum milling parameters for production of highly uniform metal-matrix nanocomposites with improved mechanical properties, *Adv. Powder Technol.*, 29(2018), No. 10, p. 2527.

[30] P. Scherrer, Estimation of the size and internal structure of colloidal particles by means of Rontgen, *N.G.W. Gottingen Math-Pys. Kl.*, 2(1918), p. 96.

[31] S.N. Danilchenko, O.G. Kukharenko, C. Moseke, I.Y. Protsenko, L.F. Sukhodub, and B. Sulkio-Cleff, Determination of the bone mineral crystallite size and lattice strain from diffraction line broadening, *Cryst. Res. Technol.*, 37(2002), No. 11, p. 1234.

[32] A. Tsuzuki, S. Sago, S.I. Hirano, and S. Naka, High temperature and pressure preparation and properties of iron carbides Fe_7C_3 and Fe_3C, *J. Mater. Sci.*, 19(1984), No. 8, p. 2513.

[33] S. Sandlöbes, M. Friák, S. Zaefferer, A. Dick, S. Yi, D. Letzig, Z. Pei, L.F. Zhu, J. Neugebauer, and D. Raabe, The relation between ductility and stacking fault energies in Mg and Mg-Y alloys, *Acta Mater.*, 60(2012), No. 6-7, p. 3011.

[34] A. Wagih, Synthesis of nanocrystalline Al_2O_3 reinforced Al

nanocomposites by high-energy mechanical alloying: Microstructural evolution and mechanical properties, *Trans. Indian Inst. Met.*, 69(2016), No. 4, p. 851.

[35] A. Wagih, Effect of Mg addition on mechanical and thermoelectrical properties of Al–Al_2O_3 nanocomposite, *Trans. Nonferrous Met. Soc. China*, 26(2016), No. 11, p. 2810.

[36] İ. Çelikyürek, N.Ö. Körpe, T. Ölçer, and R. Gürler, Microstructure, properties and wear behaviors of (Ni_3Al)p reinforced Cu matrix composites, *J. Mater. Sci. Technol.*, 27(2011), No. 10, p. 937.

[37] A. Fathy and A.A. Megahed, Prediction of abrasive wear rate of *in situ* Cu–Al_2O_3 nanocomposite using artificial neural networks, *Int. J. Adv. Manuf. Technol.*, 62(2012), No. 9-12, p. 953.

[38] M. Hou, S.H. Guo, L. Yang, J.Y. Gao, J.H. Peng, T. Hu, L. Wang, and X.L. Ye, Fabrication of Fe–Cu matrix diamond composite by microwave hot pressing sintering, *Powder Technol.*, 338(2018), p. 36.

[39] J.H. Liu, U. Khan, J. Coleman, B. Fernandez, P. Rodriguez, S. Naher, and D. Brabazon, Graphene oxide and graphene nanosheet reinforced aluminium matrix composites: Powder synthesis and prepared composite characteristics, *Mater. Des.*, 94(2016), p. 87.

[40] A. Fathy, O. Elkady, and A. Abu-Oqail, Production and properties of Cu–ZrO_2 nanocomposites, *J. Compos. Mater.*, 52(2018), No. 11, p. 1519.

[41] A. Wagih and A. Fathy, Improving compressibility and thermal properties of Al–Al_2O_3 nanocomposites using Mg particles, *J. Mater. Sci.*, 53(2018), No. 16, p. 11393.

[42] M. Alizadeh and M.M. Aliabadi, Synthesis behavior of nanocrystalline Al–Al_2O_3 composite during low time mechanical milling process, *J. Alloys Compd.*, 509(2011), No. 15, p. 4978.

[43] D. Jeyasimman, K. Sivaprasad, S. Sivasankaran, R. Ponalagusamy, R. Narayanasamy, and V. Iyer, Microstructural observation, consolidation and mechanical behaviour of AA 6061 nanocomposites reinforced by γ-Al_2O_3 nanoparticles, *Adv. Powder Technol.*, 26(2015), No. 1, p. 139.

[44] K. Chu and C.C. Jia, Enhanced strength in bulk graphene–copper composites, *Phys. Status Solidi A*, 211(2014), No. 1, p. 184.

[45] F.Y. Chen, J.M. Ying, Y.F. Wang, S.Y. Du, Z.P. Liu, and Q. Huang, Effects of graphene content on the microstructure and properties of copper matrix composites, *Carbon*, 96(2016), p. 836.

[46] C.L.P. Pavithra, B.V. Sarada, K.V. Rajulapati, T. Rao, and G. Sundararajan, A new electrochemical approach for the synthesis of copper–graphene nanocomposite foils with high hardness, *Sci. Rep.*, 4(2014), art. No. 4049.

[47] F. Shehata, A. Fathy, M. Abdelhameed, and S.F. Moustafa, Preparation and properties of Al_2O_3 nanoparticle reinforced copper matrix composites by *in situ* processing, *Mater. Des.*, 30(2009), No. 7, p. 2756.

[48] F. Shehata, A. Fathy, M. Abdelhameed, and S.F. Moustafa, Fabrication of copper–alumina nanocomposites by mechano-chemical routes, *J. Alloys Compd.*, 476(2009), No. 1-2, p. 300.

[49] M.S. Abd-Elwahed, A. Wagih, and I.M.R. Najjar, Correlation between micro/nano-structure, mechanical and tribological properties of copper–zirconia nanocomposites, *Ceram. Int.*, 46(2020), No. 1, p. 56.

[50] W.S. Barakat, A. Wagih, O.A. Elkady, A. Abu-Oqail, A. Fathy, and A. El-Nikhaily, Effect of Al_2O_3 nanoparticles content and compaction temperature on properties of Al–Al_2O_3 coated Cu nanocomposites, *Composites Part B.*, 175(2019), art. No. 107140.